STEADY DISCHARGE COEFFICIENT IN INTERNAL COMBUSTION ENGINE

Soriano, B S, soriano915@hotmail.com
Rech, C, charlesrech@uol.com.br
Automotive Mechanical Engineering Department, Lutheran University of Brazil
Av. Farroupilha, 8001, CEP , 92425-900, Canoas, RS, Brazil

Zancanaro, F V Jr, zancanaro@mecanica.ufrgs.br
Vielmo, H A, vielmoh@mecanica.ufrgs.br
Mechanical Engineering Department, Federal University of Rio Grande do Sul
Rua Sarmento Leite, 425, CEP 90050-170, Porto Alegre, RS, Brazil

Abstract. *The breathing capacity of the intake system of internal combustion engines is quantified in terms of discharge coefficient (C_D). This paper evaluates a numerical and experimental methodology to predict the discharge coefficient. Steady experimental data was obtained for various valve lift and suction pressure. The suction pressure, generated by a fan, was utilized as boundary condition for the numerical simulation. The air mass flow was measured with a commercial hot film anemometer sensor. Its characteristic curve was obtained with an standard orifice plate. The air mass sensor was connected to a data acquisition board (National Instruments 6221) and its original LabVIEW software. In order to calculate the global discharge coefficient the valve lift, refered to the angular position of the crankcase, was measured with a rotary encoder with a resolution of 0.175 degrees and a length gauge with an accuracy of ± 0.2 μm. The numerical simulation uses the commercial FLUENT 14 Finite Volumes CFD code. Regarding turbulence, computations were performed with k-ε standard model. A detailed mesh independence study was performed. The results revealed a good agreement between numerical and experimental data, with maximum relative percentage error of 3.8%.*
Keywords: *CFD, internal combustion engines, discharge coefficient.*

1. NOMENCLATURE

A	valve flow area	P_o	stagnation pressure
C_D	discharge coefficient	P_{out}	suction pressure
C_{D_Global}	global discharge coefficient	R	gas constant
I	turbulence intensity	T_o	stagnation absolute temperature
IVC	intake valve angle closing	**Greek symbols**	
IVO	intake valve angle opening	γ	specific heat ratio
l	length scale	θ	crankshaft angular position
$\dot{m}$	mass flow rate		

2.INTRODUCTION

The intake mass flow rate by an internal combustion engine (*ICE*) is one of the most important factors for an engine project. Valves and ports play an important role in the design of internal combustion engines, and influence their performance in the period they are open (Winterbone and Pearson, 1999). The steady flow data are representative of the dynamic flow behavior of the valve in an operating engine. However the pressure upstream of the valve varies significantly during the intake process, it has been shown that over the normal engine speed range, steady flow discharge coefficient results can be used to predict dynamics performance with reasonable precision (Heywood, 1988). The intake system is efficient when there is a minimal difference between the geometrical passage area and the effective flow area. This efficiency is quantified with the discharge coefficient (C_D) and represents the ratio of the geometrical passage area and the effective flow area (Ferguson, 1985).

Many numerical simulation and experimental researches were made in order to improve the breath capacity. In the experimental area Pajkovic and Petrovic (2008) utilized hot wire anemometry with 2,5 μm of diameter in order to measure the static discharge coefficient and the flow profile around the intake valve of a Diesel engine. The authors revealed that the discharge coefficient, in low lifts, is dependent of suction pressure. This is the consequence of pronounced viscous effects at low Reynolds numbers. However, with higher velocities the viscous effects become less important and the discharge coefficient doesn't depend of suction pressure. Weclas et al. (1998) also showed that at low valve lift discharge coefficient is significantly dependent of suction pressure. When valve lift is between 0.12 and 0.15 of valve diameter it is practically independent of Reynolds number. And at high valve lift discharge coefficient decreases linearly with increasing valve lift.

Regarding the numerical simulation, Paul and Ganesan (2010) performed a numerical study with *Star_CD* software and *k-ε RNG* model to compare the different intake geometry in a Diesel engine. In spite of the helical-spiral inlet geometry configuration did not achieve the best results for volumetric efficiency, the authors recommend using this shape because of the swirl ratio generation. Martins et al. (2009) with *Fluent* software and *k-ε RNG* turbulence model developed an intake system with high swirl generation for a small engine in order to promote rapid combustion.

Other papers are concerned in the validation of numerical methodology as the case of Rech et al. (2008) that analyzed the numerical methodology applied on discharge coefficient simulation of a Diesel intake system with experimental results. They utilized two different *CFD* codes, *Star_CD* and *Fluent*, and two different turbulence models: *k-ε* standard and *k-ε RNG*. The results with the best accuracy were obtained with *Star_CD* software and *k-ε RNG* model. Although, the results with the Fluent are coherent if compared with the experimental data, the difference was 6%. Recently, Rech (2010) confronted numerical and experimental results of the transient air mass flow in a *CFR* engine in order to validate the numerical methodology. Transient experimental data was obtained with a hot wire anemometer. The simulation demonstrates good agreement with measured values.

The objective of this paper is to evaluate the numerical and experimental methodology to predict a steady discharge coefficient.

3. THE DISCHARGE COEFFICIENT

The mass flow rate through a poppet valve is usually described by the equation for compressible flow through a flow restriction (Heywood, 1988). The Equation 1 relates the actual mass flow rate through the intake valve to the isentropic mass flow rate.

$$C_D = \frac{\dot{m}}{A\frac{p_o}{(RT_O)^{1/2}}\left(\frac{p_{out}}{p_o}\right)^{1/\gamma}\left\{\frac{2\gamma}{\gamma-1}\left[1-\left(\frac{p_{out}}{p_o}\right)^{\gamma-1/\gamma}\right]\right\}^{1/2}} \quad (1)$$

where $\dot{m}$ is obtained from the numerical solution, or experimentally. R is the gas (air) constant, T_o the stagnation (inlet) absolute temperature and γ the specific heat ratio. The variable A, that represents the valve flow area, is treated considering the valve lift, seat angle, inner and outer diameter as described for Blair (1999).

A global coefficient is obtaining by integration along the crankshaft angle, as follows (Rech et al., 2008):

$$C_{D\_Global} = \frac{\int_{IVO}^{IVC} C_D \, d\theta}{IVC - IVO} \quad (2)$$

where θ is a crankshaft angular position, *IVO* is the intake valve angle opening and *IVC* is the intake valve angle closing.

4. EXPERIMENTAL METHODOLOGY

Steady measurements system was made in the intake system of a standard single cylinder four stroke Honda GX35. The specifications of the engine are given in the Table 1.

Table 1. Specifications of the engine (Honda, 2012)

Honda GX35 engine	
Bore x Stroke [mm]	39 x 30
IVO/IVC [BTDC/ATDC]	25.41/66.21
Displacement [cm^3]	35.8
Maximum valve lift [mm]	2.82
Intake air system	Naturally aspirated
Compression ratio	8:1

The carburetor system was removed of the engine and the mass flow measured below the intake valve with an automotive hot film anemometer (Bosch, 2010). The incoming air dissipates heat from the hot film, so the higher the air flows, more heat is dissipated. The resulting temperature differential is a measure for the air mass flowing past the sensor. An electronic hybrid circuit evaluates this measuring data so that the air-flow quantity can be measured (Beckwith et al., 1993). Only part of the air-mass flow is registered by the sensor element. The total air mass flowing through the measuring tube is determined by means of calibration, known as the characteristic-curve of the sensor (Bosch, 2010). The characteristic-curve, relating output voltage of the hot film anemometer and the air mass flow, was

taken by an orifice plate according *ABNT* standard (NBR ISO 5167-1, 1994). The hot film anemometer was connected to a data acquisition board, National Instruments 6221 (National Instruments, 2012). With the supply of the LabVIEW software (LabVIEW, 2008), the steady measurement was done with a 2000 samples per second. The results were obtained with a mean of one minute of measurement.

In order to generate the flow in the intake system, an electrical fan controlled by a voltage variator was put at end of the cylinder providing a known suction pressure. For this test was set three different suction pressures: 10000 Pa, 8000 Pa and 6000 Pa. This pressure downstream of the valve was monitored with a piezoresistive transducer MPX5050AP (Freescale, 2010). For each suction pressure, the intake valve was opened at: 1 mm, 2 mm, 2.5 mm. The valve lift was measured with a length gauge with an accuracy of ± 0.2 μm (Heidenhain MT 25, 2012).

The intake valve opening was measured as a function of crankshaft angle to calculate the C_{D_Global}. The angular position of the crankshaft was measured with a rotary encoder with a resolution of 0.175 degree (Autonics, 2012) and the lift with the same length gauge described previously. Table 2 presents the angular interval corresponding to each intake valve lift utilized to calculate the global discharge coefficient.

Table 2. Angular interval corresponding to each intake valve lift

Intake valve lift [mm]	Angular interval $\Delta\theta$ [°]
1.000	41.967
2.000	30.059
2.500	21.929

An uncertainty study was performed to estimate the total uncertainty of the mass flow measurement system. The method utilized named *propagation of uncertainty*, proposed by Kline and McClintock (1953), consider the measurement uncertainty of each particular variable used to calculate a desired result (Beckwith et al, 1993). So the total uncertainty or the system is 4%.

5. NUMERICAL METHODOLOGY

The numerical solution was performed with *FLUENT 14* Finite Volumes *CFD* code, using *k-ε* standard turbulence model, with the High-Reynolds approach (standard wall function). The pressure-velocity coupling is solved through the SIMPLE algorithm and the differencing scheme was second order upwind. Although *k-ε* standard is not completely adequate for flow with large curvatures (Deschamps, 1998), and the flow separation after the valve, it is robust, with reasonable accuracy for a wide range of turbulent flows and popular in the automotive industry. By this reason it is also applied here.

The boundary condition at the inlet was atmospheric pressure and at outlet the desired experimental suction pressure. The mass air flow was solved for the same intake valve lift of the experimental methodology. For all cases the temperature was 296 K, the wall treated as adiabatic, turbulence intensity $I = 0.05$, and length scale $l = 0.01\ m$, as a consequence of the flow and geometrical characteristics. The convergence criteria used for residuals was 10^{-5} and all computations were performed in double precision.

Regarding the mesh, it was generated with *ICEM* (*ANSYS*) software using unstructured tetrahedral cells with three prism layers of 0.3 mm of thickness and a height ratio of 1.2. The Fig.1 shows the unstructured tetrahedral mesh in the intake wall.

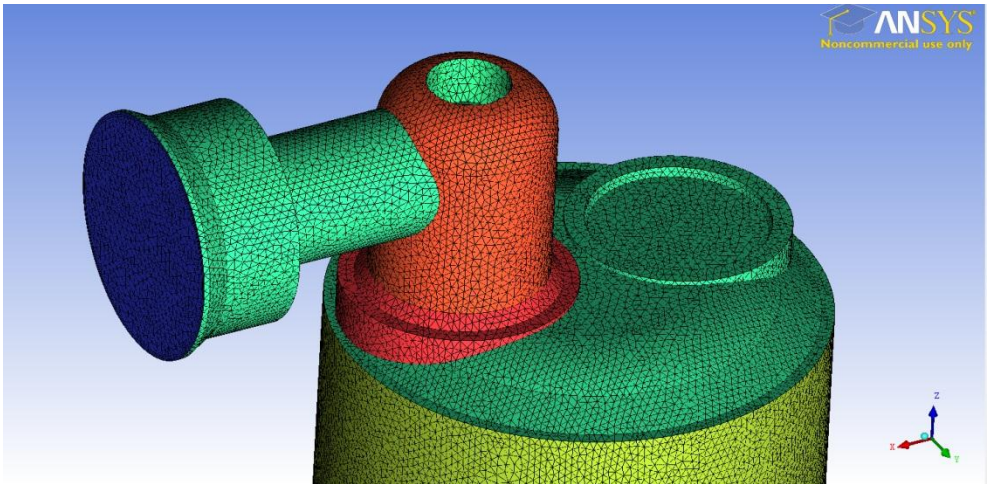

Figure 1 – unstructured tetrahedral mesh

The *k-ε* turbulence model with High-Reynolds approach requires a mesh density near the wall to assure an adequate wall treatment. Also, in regions close the valve have high gradient velocities, requiring further refinement to capture the

dynamic effects. The Fig.2 presents the density of the mesh with refinement near the wall and intake valve on the section plane A-A.

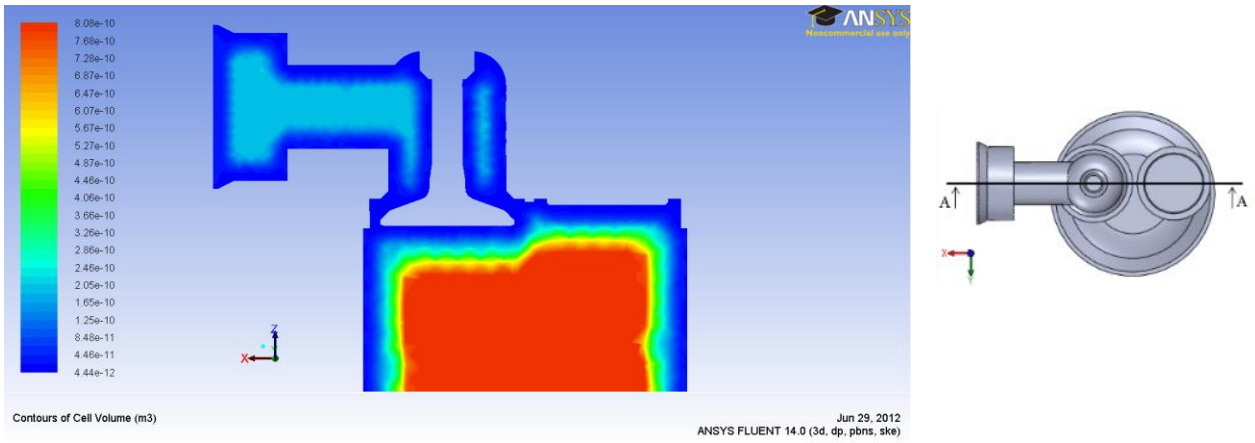

Figure 2 – Mesh density near the wall and intake valve

A mesh independence study was performed, taking as parameter the intake mass flow rate. After ten simulations with different cell numbers, was chosen about 750000 cells in the domain. As can be seen in Fig.3, after this value, the parameter varied only 0.5%.

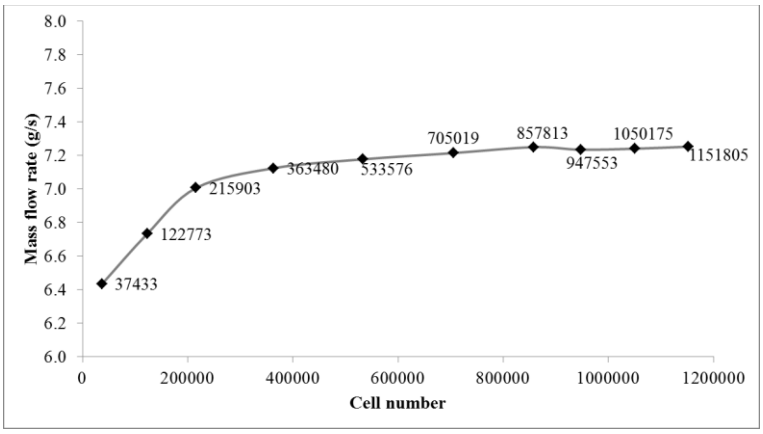

Figure 3 – Mesh independency study

6. RESULTS

Simultaneous experimental measurement and multi-dimensional numerical simulation are employed to comparison the intake discharge coefficient of the in-cylinder engine. The Fig. 4 shows the discharge coefficient, C_D, on each valve lift as a function of suction pressure. The results revealed good agreement among numerical and experimental methodology with maximum relative percentage error of 3.8% in 8000 Pa and 2 mm case.

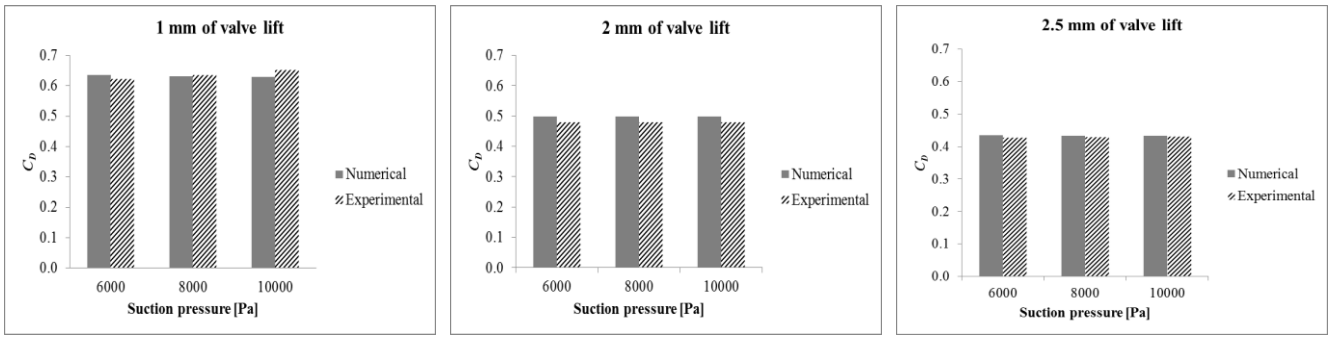

Figure 4 – Results for different valve lifts

According the results, the C_D is greater in low lifts than high valve lifts as described by other authors (Heywood, 1988; Pajkovic and Petrovic, 2008). The ICE intake port has some curves with recirculation zones and k-ε standard

model is not completely adequate. However, for global results as the case of intake mass flow rate this model presented good accuracy.

The Fig.5a shows the influence of suction pressure in experimental C_D for each valve lift. In the lower valve lift, there is a little dependence of the discharge coefficient on suction pressure, decreasing as the valve lift increases. The experimental difference between 6000 Pa and 10000 Pa in the 1.0 mm of valve lift was 4.6%. However, for higher valve lifts, the C_D is independent of suction pressures utilized, with the maximum difference of 0.9% in 2.5 mm of valve lift. The Fig.5b compares the numerical solution and experimental measurement, where it possible to note that good agreement with maximum error obtained was 2.3%.

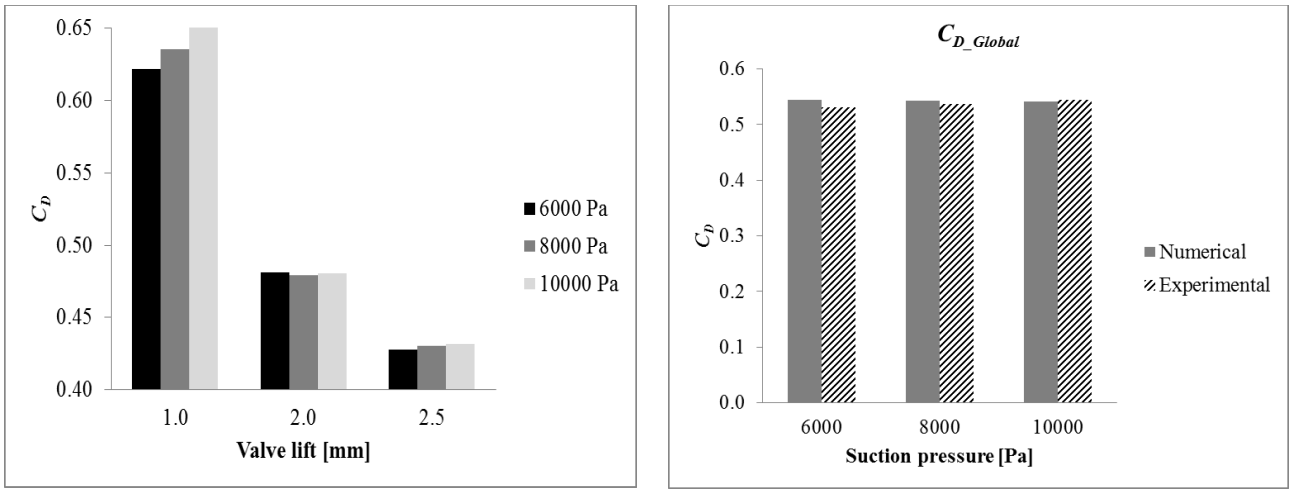

(a) (b)

Figure 5 – (a) Comparison of C_D between different suction pressures, (b) C_{D_Global} for different suction pressures

The Fig.6-8 show the velocity vectors for different valve lift and 10000 Pa of suction pressure in the section plane A-A. A large recirculation zone is detected below valve in all lifts and suction pressures tested, caused by the valve downstream low pressure. This phenomenon is dependent of valve lift, moving to the right side of the cylinder as the valve closes.

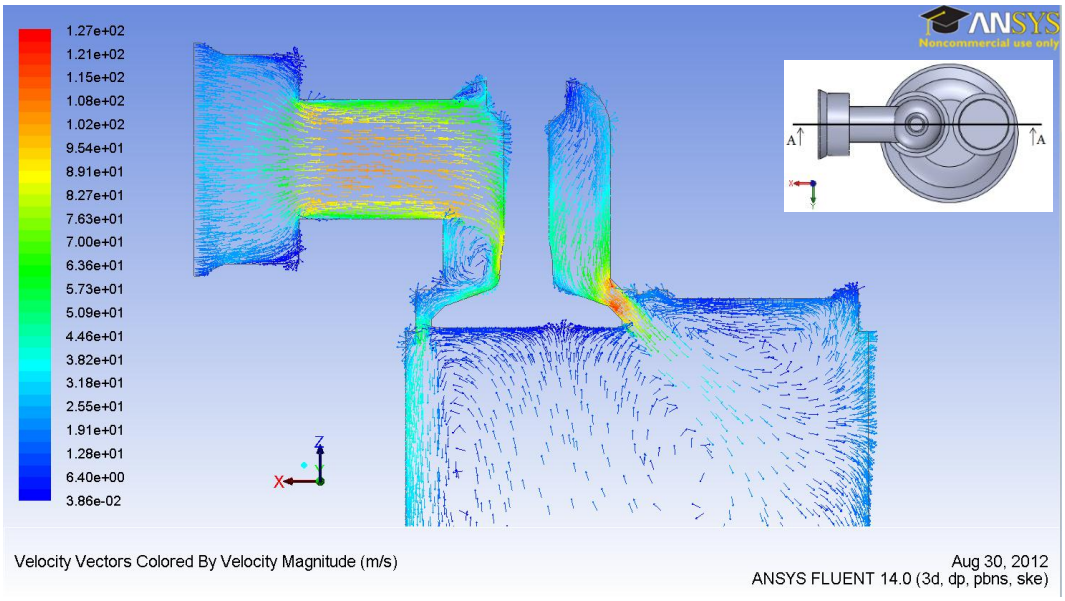

Figure 6 – Velocity vectors on the cut A-A for 2.5 mm of lift

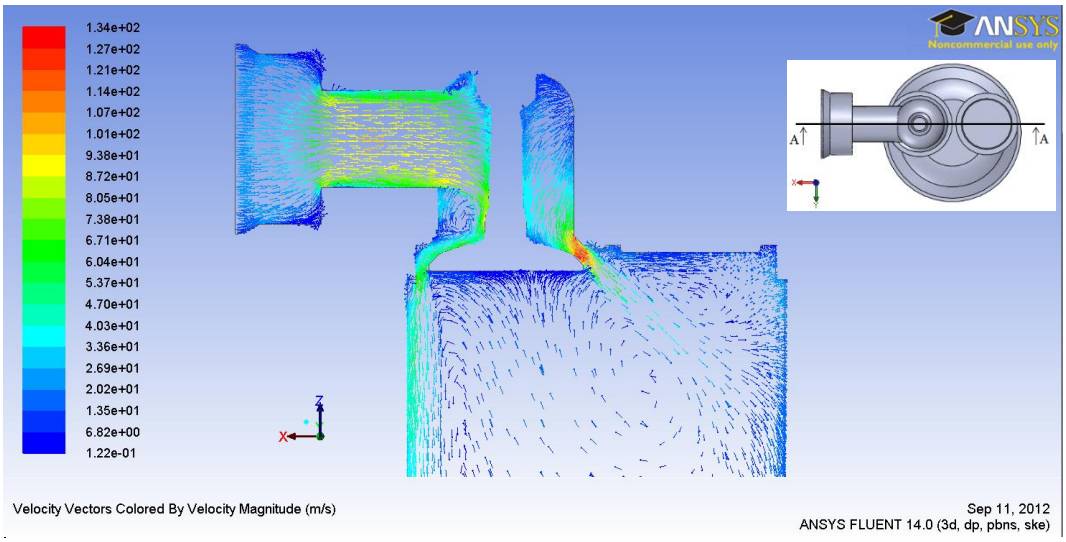

Figure 7 – Velocity vectors on the cut A-A for 2 mm of lift

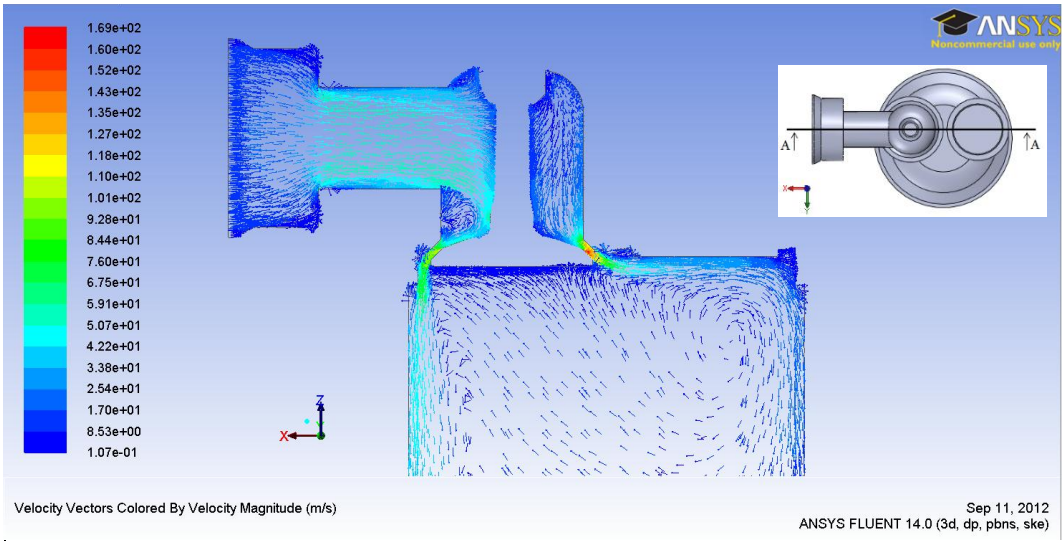

Figure 8 – Velocity vectors on the cut A-A for 1 mm of lift

As can be seen in the Fig.9, the distribution of the flow around the valve gap is irregular for all cases, causing a reduction of discharge coefficient. It is also detected recirculation zone in the intake duct caused by a sharp edge shape of the duct. This phenomenon causes a pressure drop in the intake system and decreases the discharge coefficient.

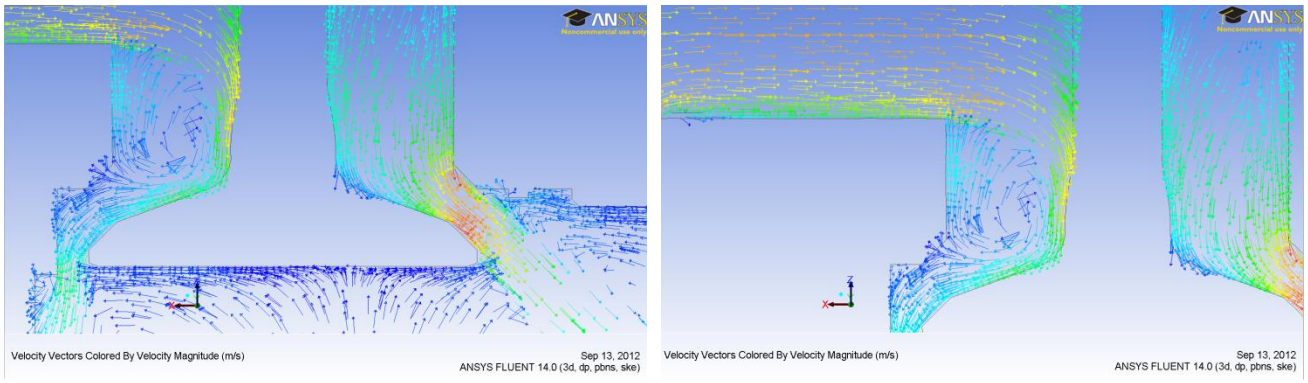

Figure 9 – Velocity vectors on the cut A-A for 2.5 mm of lift in detail

The Fig.10 shows the absolute pressure contours for 2.5 mm of valve lift and 10000 Pa of suction pressure in the section plane A-A. It is possible to observe that lowest values are concentrated around the intake valve plate because high velocities.

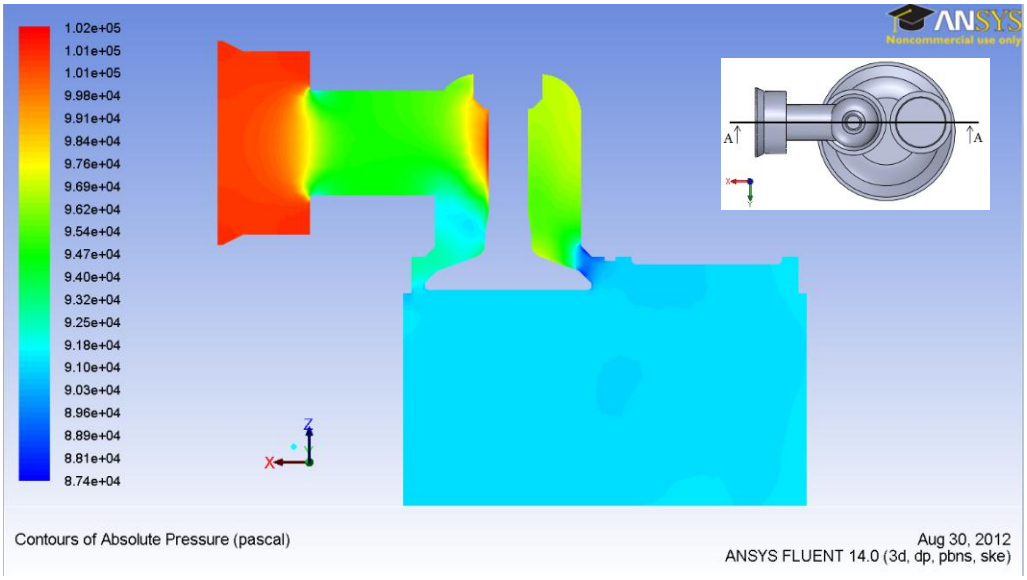

Figure 10 – Pressure field at 2.5 mm valve lift and 10000 Pa pressure suction on the cut A-A

The Fig.11 shows the turbulent kinetic energy contours, for 2.5 mm of valve lift and 10 kPa of suction pressure, in the section plane A-A The intake port, steam valve left face, and valve seat are the principal source of turbulent kinetic energy production, associated with high velocity gradients. Downstream the valve, the turbulence energy decays, due to expansion, as expected.

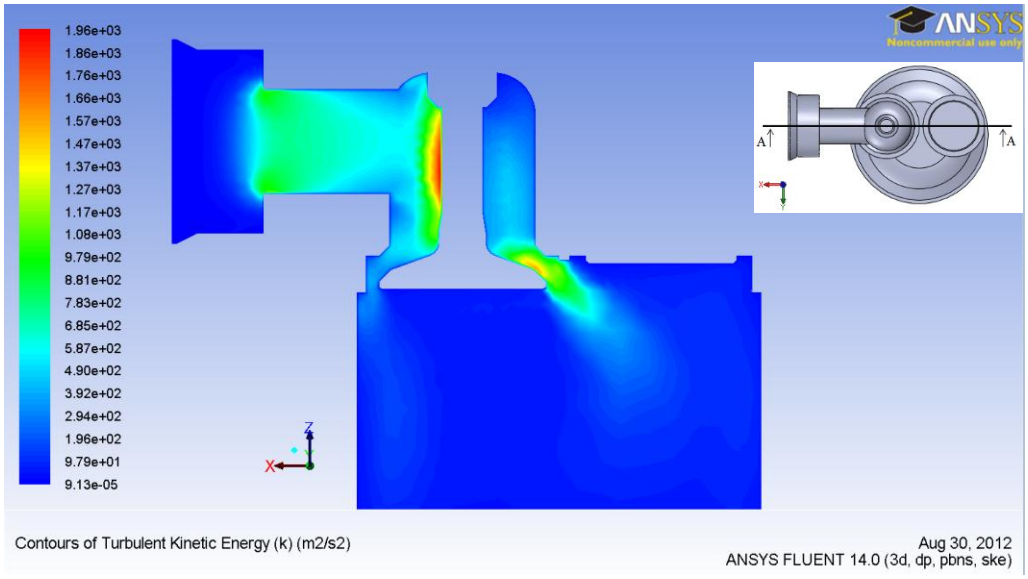

Figure 11 – Turbulent kinetic energy on the cut A-A

7. CONCLUSION

The steady flow through the intake system of a single cylinder, four strokes, was solved with *FLUENT 14* Finite Volumes *CFD* code, applying the k-ε standard turbulence model. The numerical results were compared, for three different valve lift and suction pressures, with experimental results using an automotive hot film anemometer sensor, calibrated through an orifice plate.

The results revealed a good agreement, with a maximum relative percentage error of 3.8%, for a suction pressure of 8 kPa and 2 mm of valve lift. So, both applied methodologies can be used to predict the steady discharge coefficient.

It was verified that the discharge coefficient is more dependent of suction pressure in low valve lift. To 1 mm of valve lift the C_D variation with suction pressure was 4.6% in the experimental results, in the case of 2.5 mm the variation was 0.9%. The C_D decreases with the increase of valve lift.

A recirculation zone, detected in the last part of the intake duct, associated with the irregular distribution of the flow around the valve gap, contributes to reduce the discharge coefficient.

8. ACKNOWLEDGEMENTS

Zancanaro, F V Jr thanks the CNPq for the doctoral grant, and Vielmo H A thanks CNPq for research grant 302503/2009-9, and for CNPq Universal Project 470325/2011-9.

The authors thank the financial support from ULBRA Research, Brazil, through a scientific productivity grant to Rech, C. and the Energetic Efficiency Project. Also a scientific initiation program scholarship grant to Soriano, B. S.

9. REFERENCES

ANSYS FLUENT, Theory Guide, 2011.

Associação Brasileira de Normas Técnicas. NBR ISO 5167-1: Medição de vazão de fluidos por meio de instrumentos de pressão – Parte 1: Placas de orifício, bocais e tubos de Venturi instalados em seção transversal circular de condutos forçados. Rio de Janeiro, 1994.

Autonics rotary encoder (incremental type), 2012, "E40S-6-2048-6-L-5 manual". http://autonics.thomasnet.com/Asset/E40S,HB,E80H%20manual.pdf

Beckwith, T. G.; Marangoni, R. D.; Leinhard, J.H. "Mechanical Measurements", 5. ed., 1993.

Blair, G. P., Design and Simulation of Four Stroke Engines. SAE International, 1999.

Bosch, 2010 "Hot-film air-mass meter, type HFM 2" model 0 280 218 002 http://apps.bosch.com.au/motorsport/downloads/sensors_airmass.pdf.

Deschamps, C. J. . Modelos Algébricos e Diferenciais. In: A.P.S. Freire, P.P.M. Menut e S. Jian. (Org.). I Transição e Turbulência. Rio de Janeiro / RJ: ABCM. 1998, v. 1, p. 99-155.

Ferguson, Colin R., Internal combustion engine. New York: J. Wiley, 1985.

Freescale semiconductor. Integrated silicon pressure sensor on-chip signal conditioned, temperature compensated and calibrated, 2010. http://www.freescale.com/files/sensors/doc/data_sheet/MPX5050.pdf

Heywood, J.B. 1988, Internal Combustion Engines. McGraw-Hill Inc.

High-accuracy length gauges, 2012, "HEIDENHAIN-METRO MT25", https://www.valuetronics.com/Manuals/HEIDENHAIN_MT12-MT25B.pdf.

Honda Engines GX35, 2012, "model-detail/gx35" http://engines.honda.com/models/model-detail/gx35.

Kanoto, Y., Nagai, K., Kawa T., Iida, N., 2011"Cycle-to-Cycle Flow Rate Measurement on Reciprocating HCCI Engine Using Fast-Response Laminar Flow Meter". Journal of Environment and Engineering, Vol. 6, No. 1.

Kline, S. J.; McClintock, F. A. Describing uncertainties in single-sample experiments. Mech. Engr. 75:3-8, 1953.

Krishna, B. M., Bijucherian, A., Mallikarjuna, J. M., 2010 "Effect of Intake Manifold Inclination on Intake Valve Flow Characteristics of a Single Cylinder Engine using Particle Image Velocimetry". International Journal of Engineering and Applied Sciences, 6:2.

Labview, 2008 "User guide" National Instruments.

Martins, J.; Teixeira, S; Coene, S. "Design of an inlet track of a small I.C. engine for swirl enhancement", 20th International Congress of Mechanical Engineering, Gramado – RS. Proceedings of COBEM 2009, Rio de Janeiro, RJ: ABCM, 2009.

National instruments, 2012, "NI PCI-6221". http://sine.ni.com/nips/cds/print/p/lang/en/nid/14132.

Pajkovic, V. R, Petrovic, S. V. Spatial flow velocity distribution around an inlet port/valve annulus. THERMAL SCIENCE: Vol. 12 (2008), No. 1, pp. 73-83.

Paul, B., Ganesan, V., 2010, "Flow field development in a direct injection diesel engine with different manifolds". International Journal of Engineering, Science and Technology. Vol. 2, No. 1, pp. 80-91.

Rech, C., 2010, "Análise Numérica e Experimental do Escoamento em Motores de Combustão Interna." Tese (Doutorado em Engenharia Mecânica) – Programa de Pós-Graduação em Engenharia Mecânica, Universidade do Rio Grande do Sul. Porto Alegre.

Rech, C.; Baratta, M.; Catania, A.E.; Pesce, F.C.; Spessa, E.; Vielmo, H.A. "Comparisons Between Steady State Analyses of a High Swirl-Generating Helical Intake Port for Diesel Engines", 12th Brazilian Congress of Thermal Engineering and Sciences, Belo Horizonte - MG. Proceedings of ENCIT, Rio de Janeiro, RJ: ABCM, 2008.

Weclas, M.; Melling, A.; Durst, F. Flow separation in the inlet valve gap of piston engines. Prog. Energy Combust. Sci. Vol. 24, pp. 165-195. 1998.

Winterbone D.E., R.J. Pearson, Design Techniques for Engine Manifolds – Wave action methods for IC engines, SAE International, USA, 1999.

10. RESPONSIBILITY NOTICE

The authors are the only responsible for the printed material included in this paper.